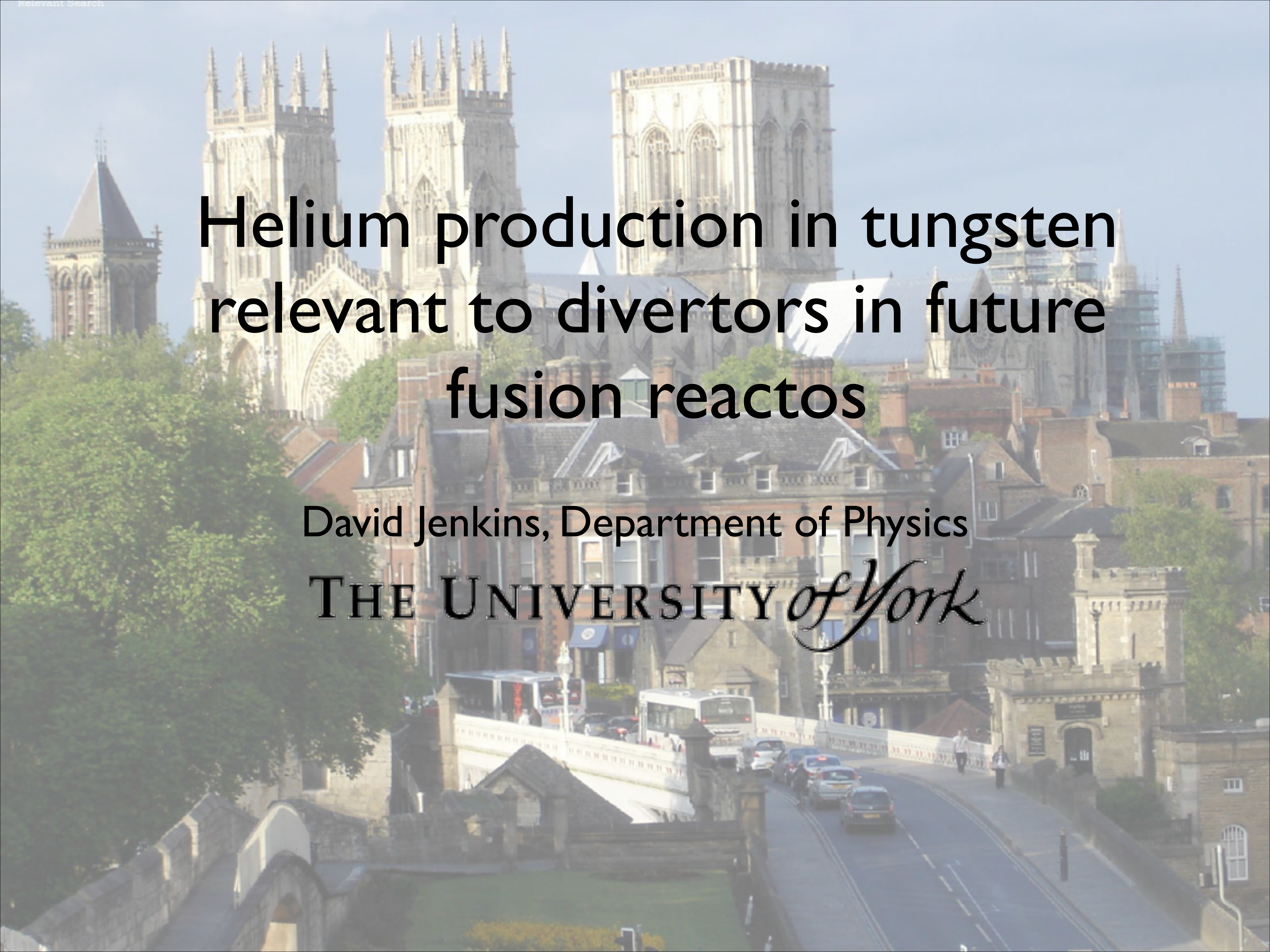

Helium production in tungsten relevant to divertors in future fusion reactos

David Jenkins, Department of Physics

THE UNIVERSITY of York

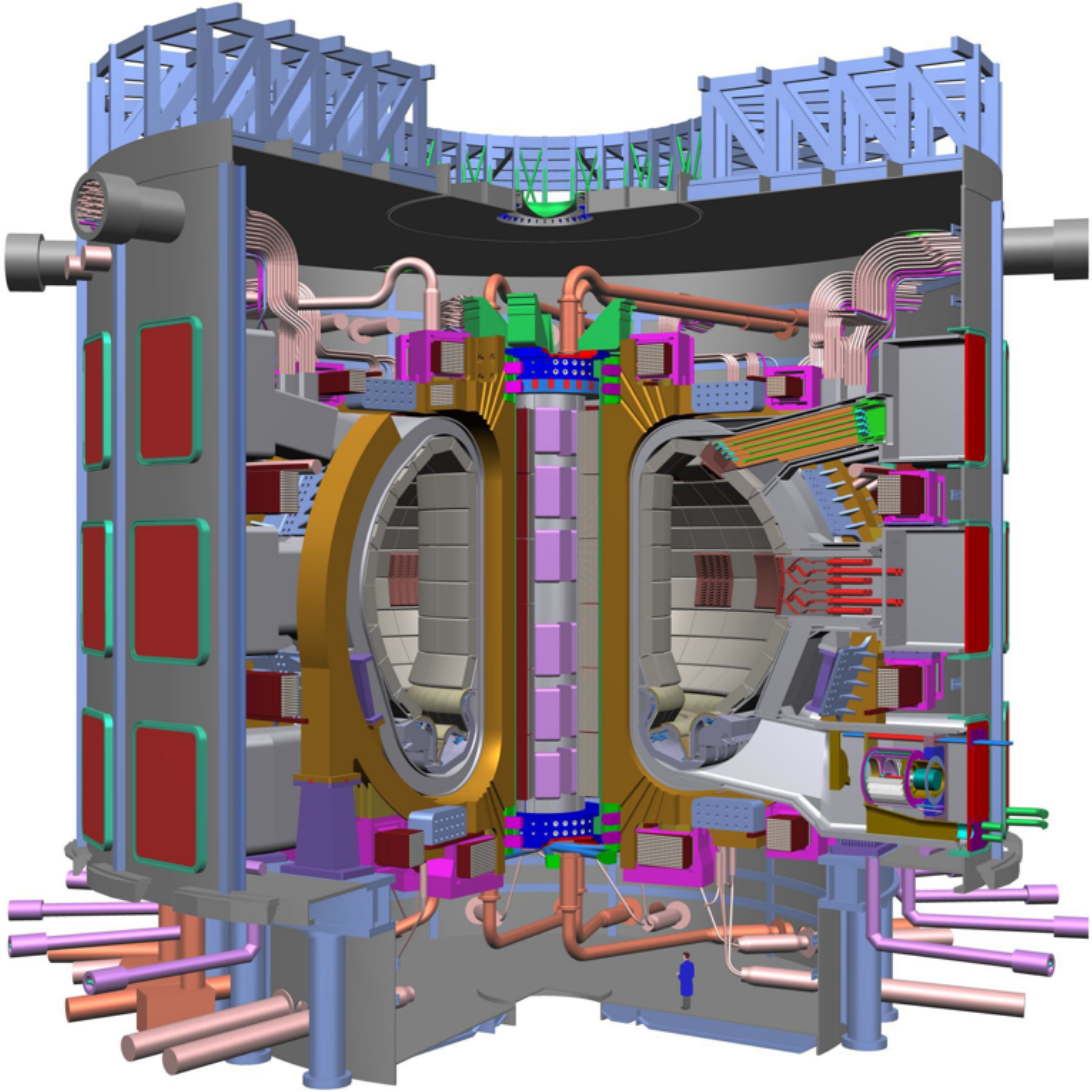

CCFE-PR(12)02

M.R. Gilbert, S.L. Dudarev, S. Zheng, L.W. Packer, and J.-Ch. Sublet

Transmutation, gas production, and helium embrittlement in materials under neutron irradiation.

ABSTRACT.

The high-energy, high-intensity neutron fluxes produced by the fusion plasma will have a significant life-limiting impact on reactor components in both experimental and commercial fusion devices. As well as producing defects, the neutrons bombarding the materials initiate nuclear reactions, leading to transmutation of the elemental atoms. Products of many of these reactions are gases, particularly helium and hydrogen, which cause swelling and embrittlement of materials. This paper investigates, using both neutron-transport and inventory calculations, the variation in nuclear transmutation and gas production rates at various locations of a conceptual design of the next-step fusion device DEMO. Modelling of grain structures and gas diffusion rates illustrates that the timescale for susceptibility to helium embrittlement varies widely between different materials, and between the same materials situated at different locations in the DEMO structure.

M.R. Gilbert et al., J. Nucl. Materials 442, S755 (2013)

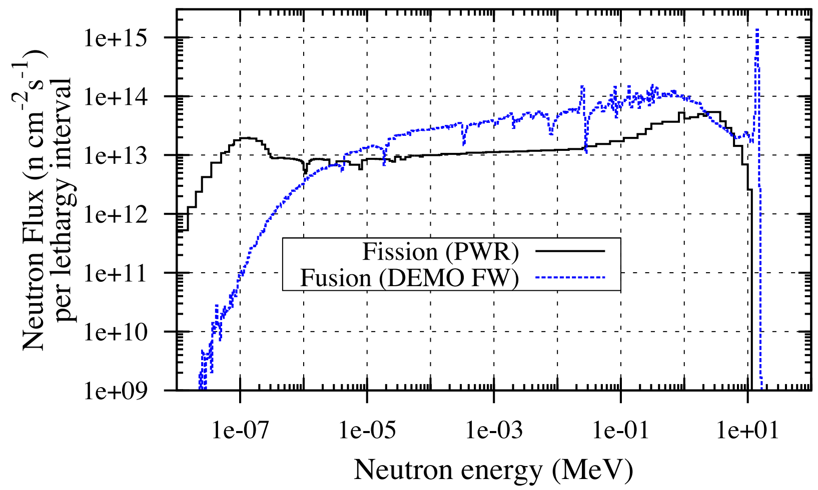

Figure 1. Comparison of the neutron-energy spectra in fission and fusion reactors. For fission the average neutron spectrum in the fuel-assembly of a PWR reactor is shown, while the equatorial FW spectrum for the DEMO model in figure 2 is representative of fusion.

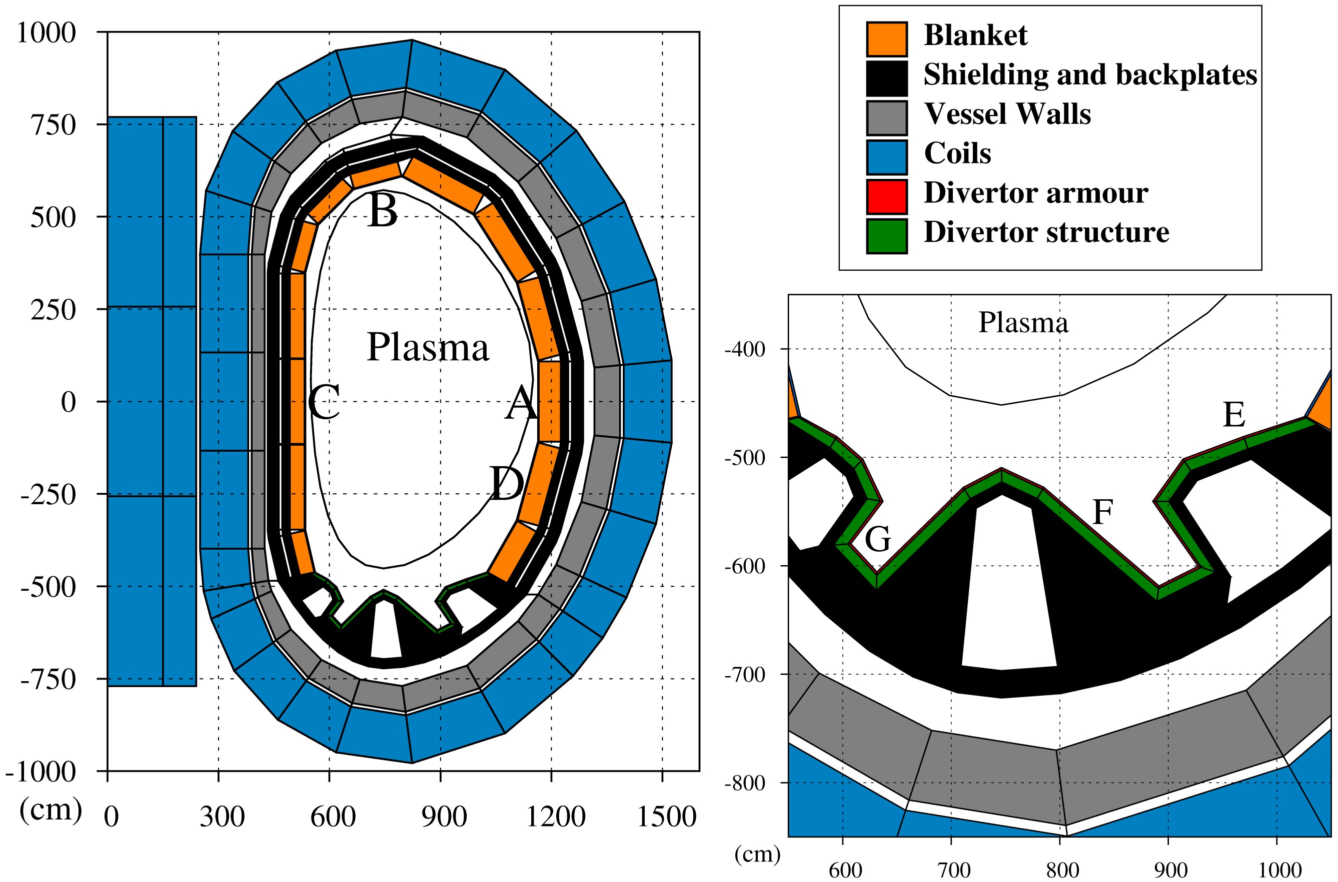

Figure 2. The simplified, homogeneous, DEMO model used in MCNP simulations to obtain neutron fluxes and spectra.

The divertor is one of the key components of the ITER machine. Situated along the bottom of the vacuum vessel, its function is to extract heat and helium ash — both products of the fusion reaction — and other impurities from the plasma, in effect acting like a giant exhaust system. It will comprise two main parts: a supporting structure made primarily from stainless steel, and the plasma-facing components, weighing about 700 tons. The plasma-facing components will be made of tungsten, a high-refractory material.

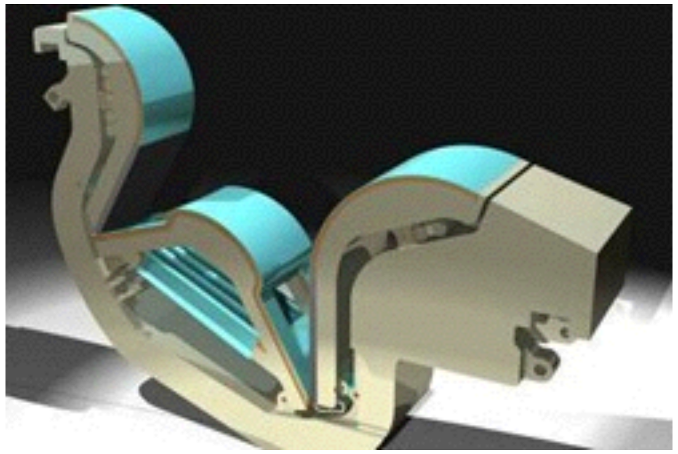

Materials damage:

- Displacement of atoms in the lattice by fast neutrons
- Transmutation of elements in the materials
- Production of gas within the material
- Combined effect of neutrons and plasma?

Impurities produced in W following neutron irradiation in DEMO

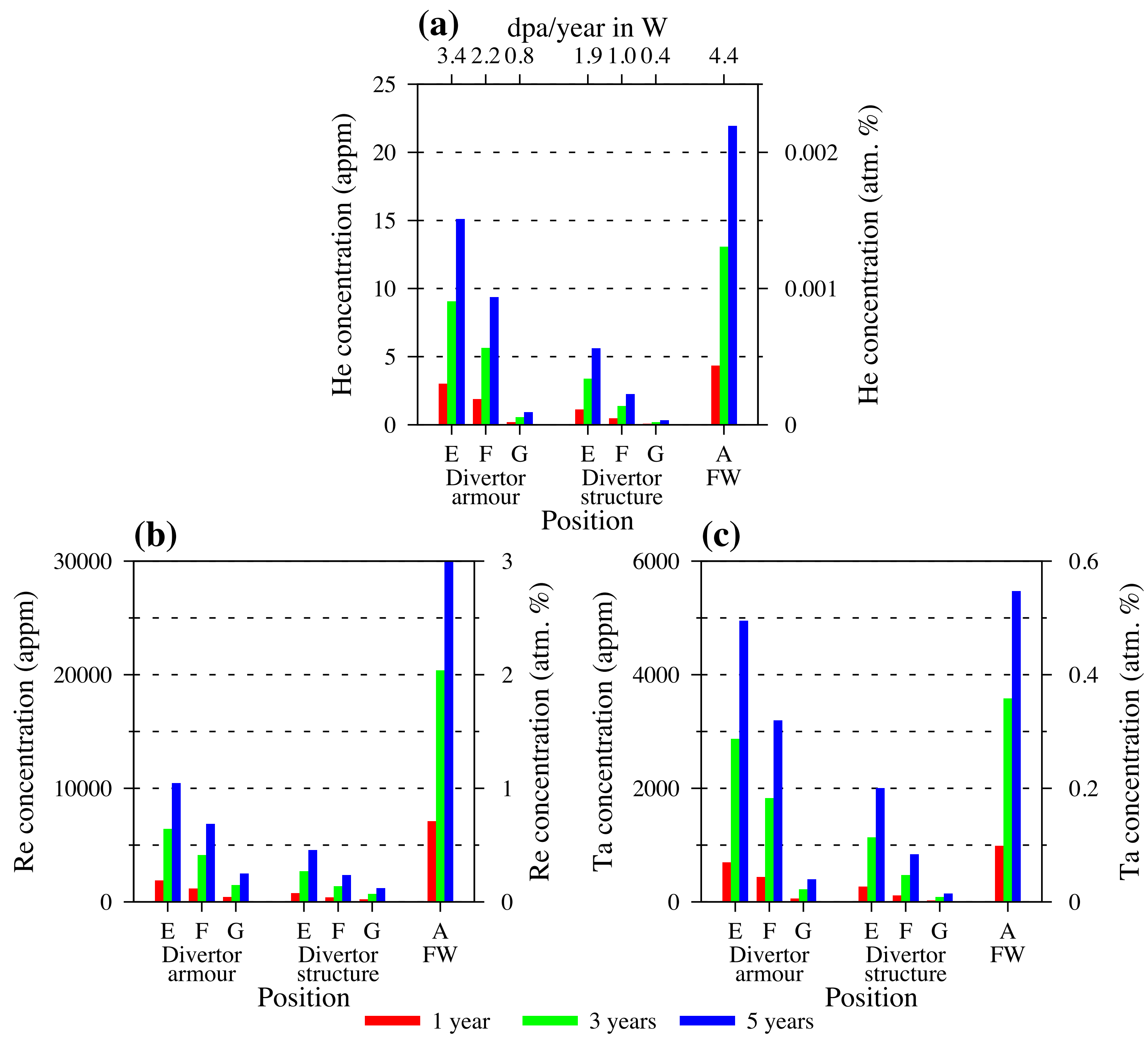

calculated using neutron transport and FISPACT inventory code

He produced from (n,a); Re from (n,g) and Ta from e.g. (n,2n)

Table 2. Table of calculated critical boundary densities ν^c_{He}, critical bulk concentrations G^c_{He} for He in various elements, and the approximate critical lifetimes t^c in DEMO first-wall full-power time and equivalent integral dpa. Results for two different grain radii R shown.

Element	ν^c_{He} (cm^{-2})	R (μm)	G^c_{He} (appm)	DEMO FW t^c	DEMO FW dpa^c
Fe	6.76×10^{14}	5	47.8	4 months	4.79
V	8.59×10^{14}	5	71.3	1.5 years	25.07
Cr	5.53×10^{14}	5	39.9	5 months	6.27
Mo	7.31×10^{14}	5	68.4	1.5 years	14.34
Nb	8.96×10^{14}	5	96.8	2.5 years	39.99
Ta	9.25×10^{14}	5	100.1	21 years	118.92
W	7.51×10^{14}	5	71.4	16 years	71.11
Be	4.80×10^{14}	5	23.3	4 days	0.08
Zr	8.82×10^{14}	5	123.2	4 years	61.99
Fe	6.76×10^{14}	0.5	478.1	4 years	57.47
V	8.59×10^{14}	0.5	713.2	15 years	250.75
Cr	5.53×10^{14}	0.5	398.6	4 years	60.20
Mo	7.31×10^{14}	0.5	684.1	16 years	152.97
Nb	8.96×10^{14}	0.5	968.2	21 years	335.92
Ta	9.25×10^{14}	0.5	1001.2	283 years	1602.62
W	7.51×10^{14}	0.5	714.3	244 years	1084.49
Be	4.80×10^{14}	0.5	233.0	22 days	0.43
Zr	8.82×10^{14}	0.5	1231.7	40 years	619.88

ENDF/B-VII.1 Nuclear Data for Science and Technology: Cross Sections, Covariances, Fission Product Yields and Decay Data

M.B. Chadwick,[1,*] M. Herman,[2] P. Obložinský,[2] M.E. Dunn,[3] Y. Danon,[4] A.C. Kahler,[1] D.L. Smith,[5] B. Pritychenko,[2] G. Arbanas,[3] R. Arcilla,[2] R. Brewer,[1] D.A. Brown,[2,6] R. Capote,[7] A.D. Carlson,[8] Y.S. Cho,[13] H. Derrien,[3] K. Guber,[3] G.M. Hale,[1] S. Hoblit,[2] S. Holloway,[1] T.D. Johnson,[2] T. Kawano,[1] B.C. Kiedrowski,[1] H. Kim,[13] S. Kunieda,[1,15] N.M. Larson,[3] L. Leal,[3] J.P. Lestone,[1] R.C. Little,[1] E.A. McCutchan,[2] R.E. MacFarlane,[1] M. MacInnes,[1] C.M. Mattoon,[6] R.D. McKnight,[5] S.F. Mughabghab,[2] G.P.A. Nobre,[2] G. Palmiotti,[14] A. Palumbo,[2] M.T. Pigni,[3] V.G. Pronyaev,[9] R.O. Sayer,[3] A.A. Sonzogni,[2] N.C. Summers,[6] P. Talou,[1] I.J. Thompson,[6] A. Trkov,[10] R.L. Vogt,[6] S.C. van der Marck,[11] A. Wallner, [12] M.C. White,[1] D. Wiarda,[3] P.G. Young[1]

[1] *Los Alamos National Laboratory, Los Alamos, NM 87545, USA*
[2] *Brookhaven National Laboratory, Upton, NY 11973-5000, USA*
[3] *Oak Ridge National Laboratory, Oak Ridge, TN 37831-6171, USA*
[4] *Rensselaer Polytechnic Institute, Troy, NY 12180, USA*
[5] *Argonne National Laboratory, Argonne, IL 60439-4842 USA*
[6] *Lawrence Livermore National Laboratory, Livermore, CA 94551-0808, USA*
[7] *International Atomic Energy Agency, Vienna-A-1400, PO Box 100, Austria*
[8] *National Institute of Standards and Technology, Gaithersburg, MD 20899-8463, USA*
[9] *Institute of Physics and Power Engineering, Obninsk, Russian Federation*
[10] *Jozef Stefan Institute, Jamova 39, 1000 Ljubljana, Slovenia*
[11] *Nuclear Research and Consultancy Group, P.O. Box 25, NL-1755, ZG Petten, The Netherlands*
[12] *Faculty of Physics, University of Vienna, Waehringer Strasse 17, A-1090 Vienna, Austria*
[13] *Korea Atomic Energy Research Institute, Daejeon, Korea*
[14] *Idaho National Laboratory, Idaho Falls, ID 83415, USA and*
[15] *Japan Atomic Energy Agency, Tokai-mura Naka-gun, Ibaraki 319-1195, Japan*

(Received 12 July 2011; revised received 22 September 2011; accepted 17 October 2011)

However, the previous VII.0 data were considered unsatisfactory during recent data validation and assessments: systematic discrepancies were observed in criticality safety benchmarks containing tungsten [6], fusion neutronics benchmarks [102], and measured constants for neutron activation [103]. In addition, new experimental data have been measured (*e.g.* total cross section data for natural tungsten measured by Abfalterer *et al.* in 2001 [104], total cross section data for separated tungsten isotopes measured by Dietrich *et al.* in 2003 [105], and several sets of charged-particle emission cross sections). Finally, there was no evaluation available for neutron induced reactions on the ^{180}W isotope. These deficiencies, together with the availability of new data in the fast neutron range, motivated the work presented herein. Results of comprehensive experimental data analysis and VII.1 evaluations for neutron interactions on tungsten isotopes ^{180,182,183,184,186}W in the neutron energy range up to 150 MeV [106, 107] are described below.

EPJ Web of Conferences **42**, 02002 (2013)
DOI: 10.1051/epjconf/20134202002

Evaluation of stable tungsten isotopes in the resolved resonance region

F. Emiliani[1], K. Guber[2], S. Kopecky[1], C. Lampoudis[1], C. Massimi[3], P. Schillebeeckx[1], K. Volev[1,4]

[1]European Commission, Joint Research Centre, Institute for Reference Materials and Measurements (IRMM), Retieseweg 111, B-2440 Geel, Belgium
[2]Oak Ridge National Laboratory, Oak Ridge, USA, TN-37831
[3]Department of Physics, University of Bologna and sezione INFN of Bologna, Via Irnerio 46, Bologna, 40126 Italy
[4]Institute for Nuclear Research and Nuclear Energy (INRNE), Sofia, Bulgaria

Abstract. In the last decade benchmark experiments and simulations, together with newly obtained neutron cross section data, have pointed out deficiencies in evaluated data files of W isotopes. The role of W as a fundamental structural material in different nuclear applications fully justifies a new evaluation of $^{182, 183, 184, 186}$W neutron resonance parameters. In this regard transmission and capture cross section measurements on natural and enriched tungsten samples were performed at the GELINA facility of the EC-JRC-IRMM. A resonance parameter file used as input in the resonance shape analysis was prepared based on the available literature and adjusted in first instance to transmission data.

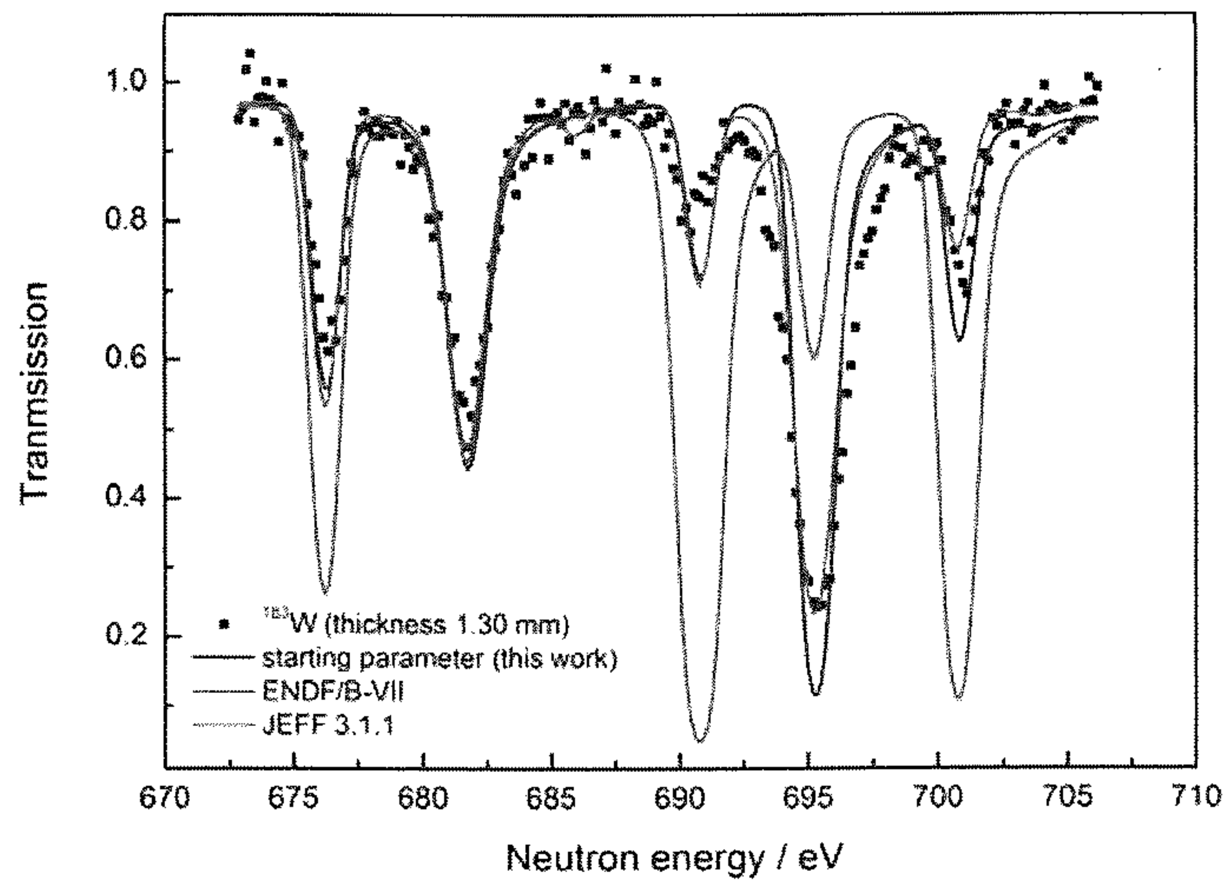

$^{186}W(n,\alpha)^{183}Hf$

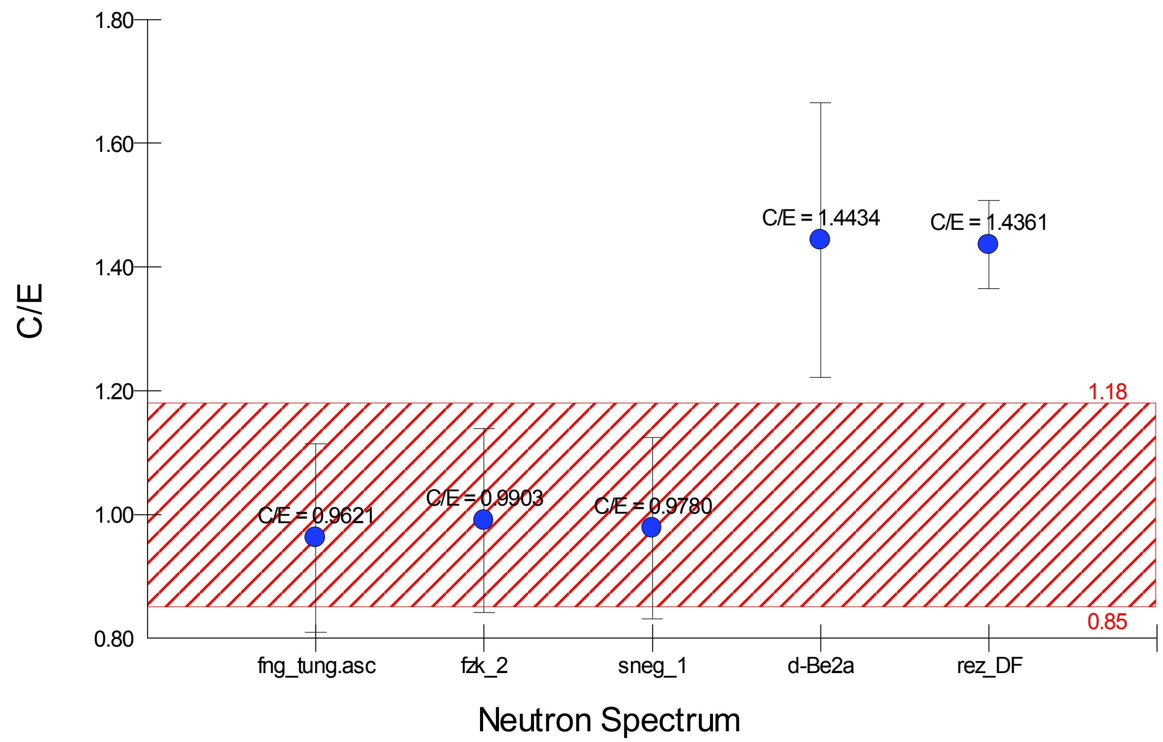

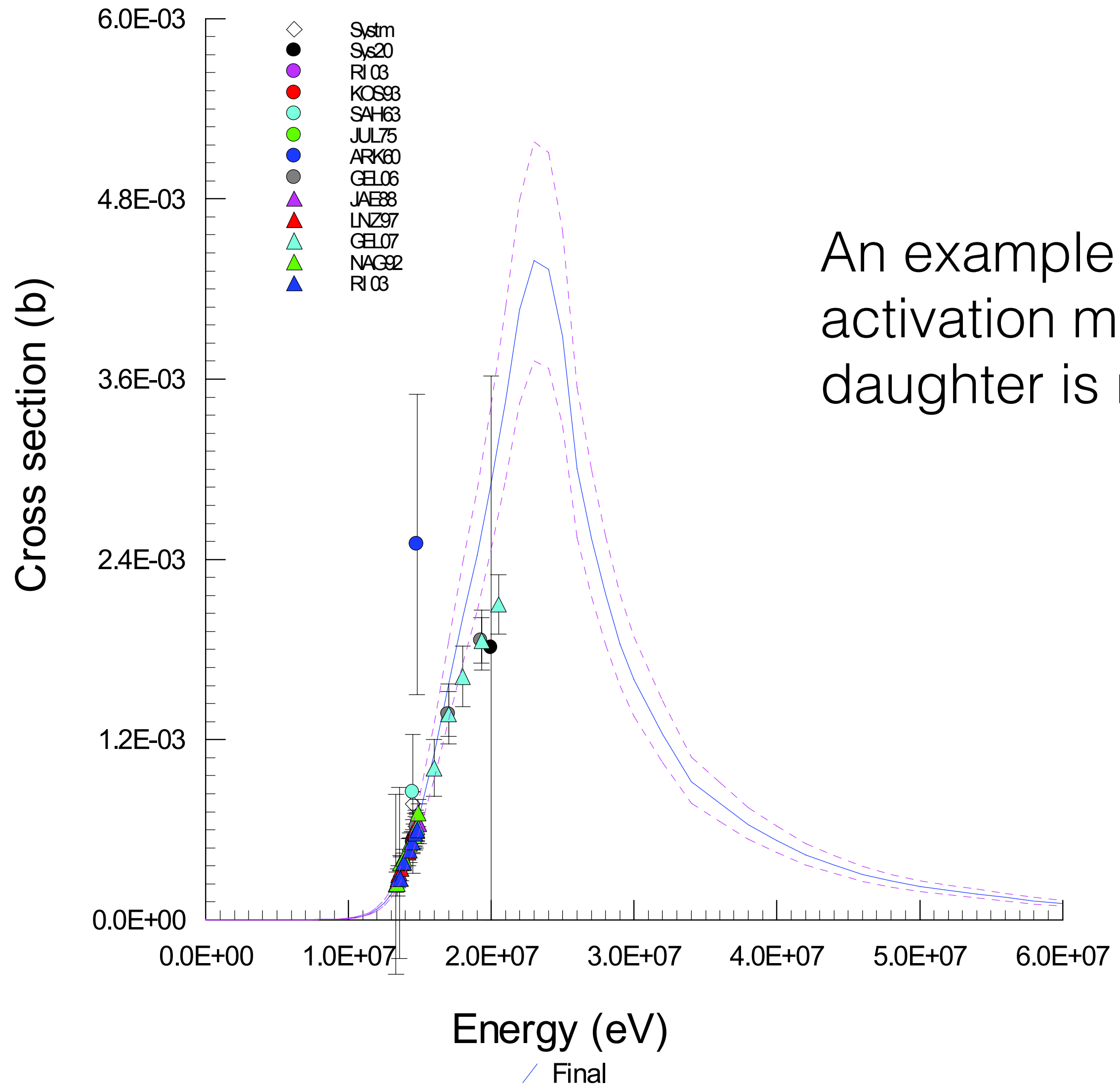

An example well-constrained through activation measurements because daughter is radioactive

$^{182}W(n,\alpha)^{179n}Hf$

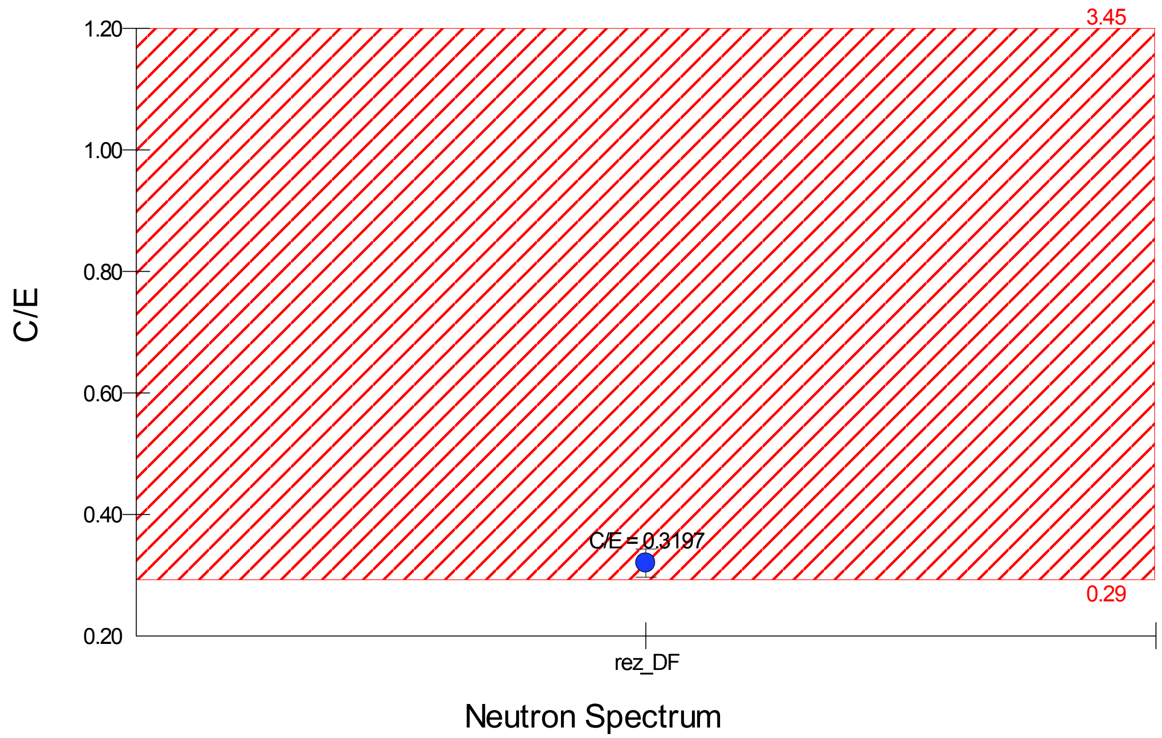

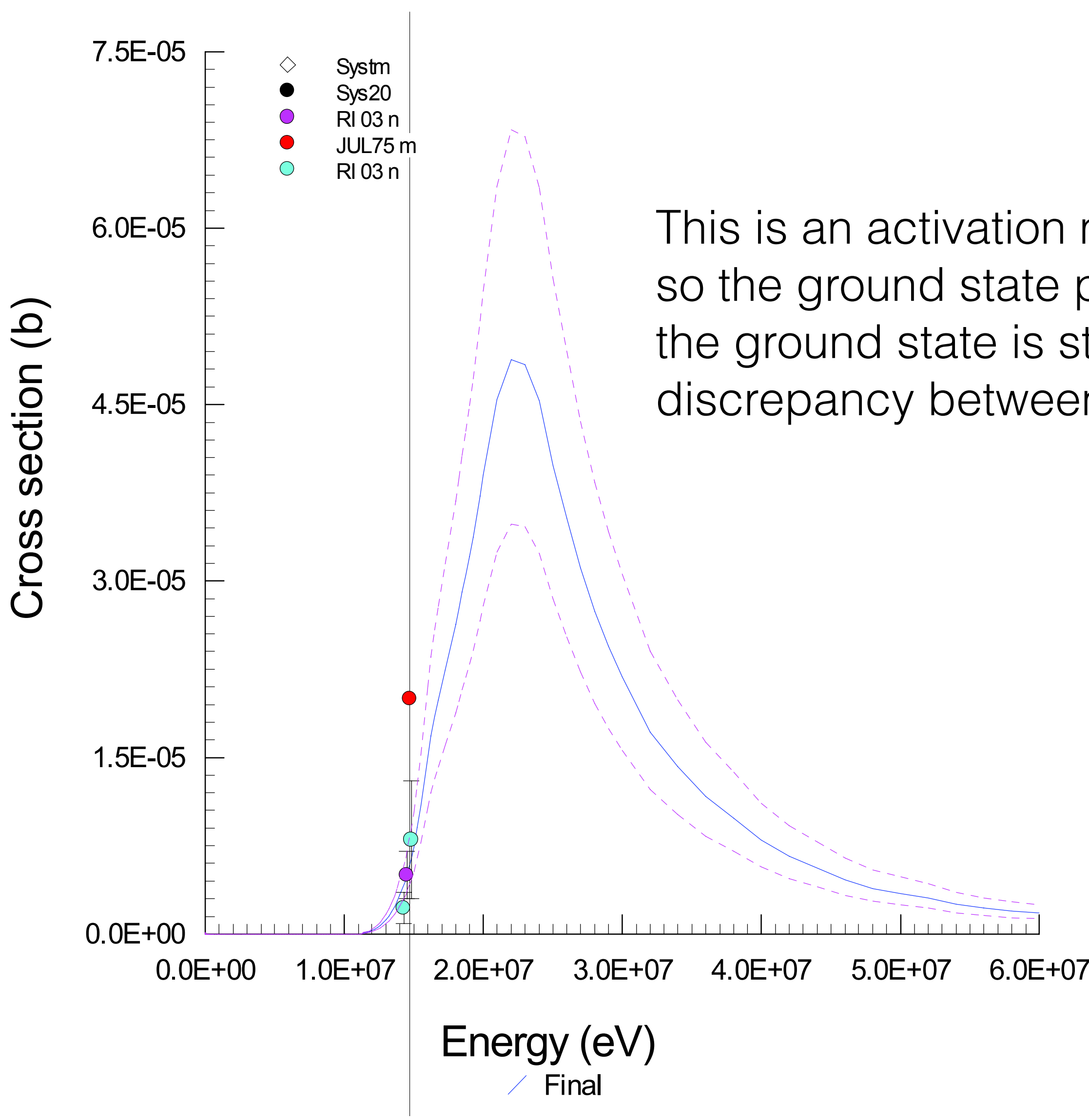

This is an activation measurement
so the ground state part is missing because the
the ground state is stable. Even so, there is quite some
discrepancy between calculated and evaluated data.

Kinematics for typical W(n,a) reactions

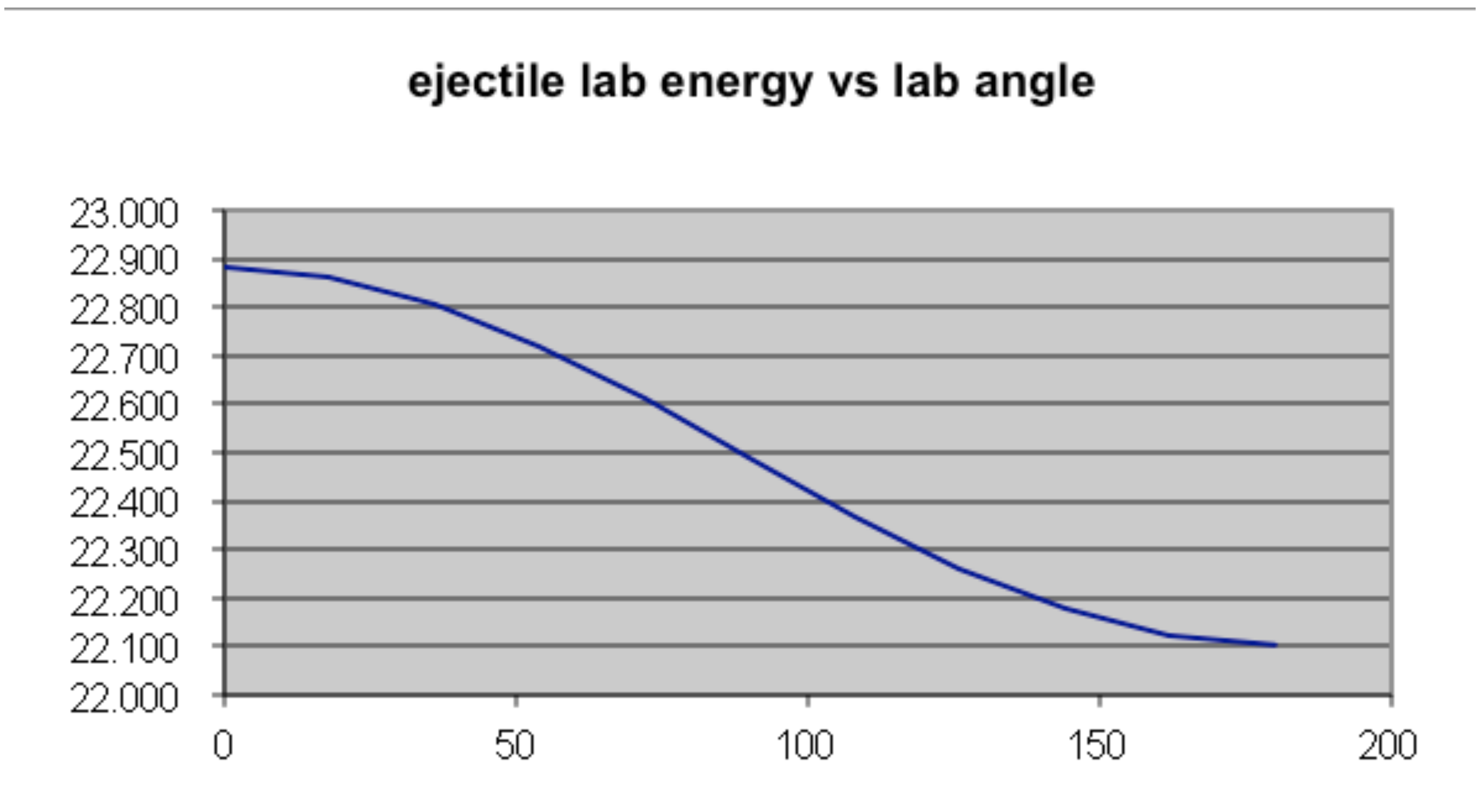

Cross-sections are millibarns
Energies of particles quite high
BUT relevant neutron energies in challenging region

Detection of (n,α) reactions

The main problem in (n,α) measurements is the background from other reactions in the sample, or in the detectors (gas recoils, etc.)

Micromegas chamber (MGAS)

- low-noise, high-gain
- Several samples in parallel

Diamond (pCVD or sCVD)

- Background reactions only above 1 Mev
- Very fast response
- Particle discrimination (if sCVD or charge collection distance > 300 μm)

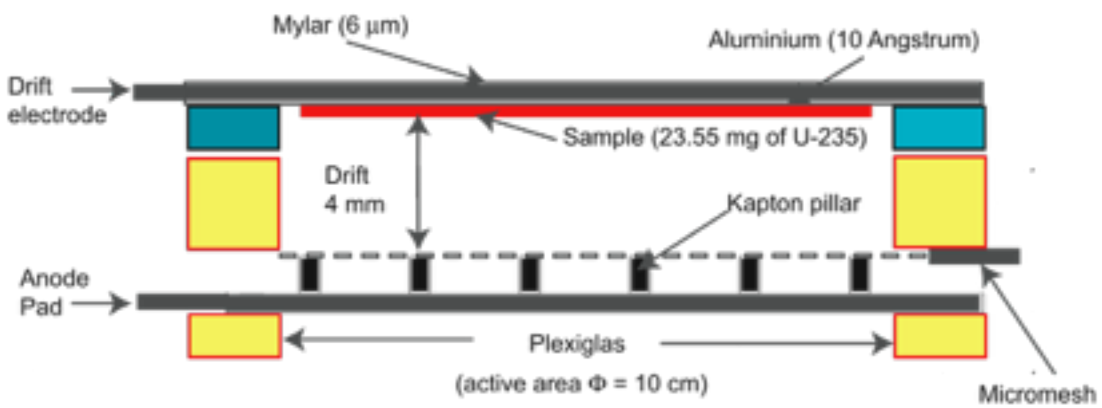

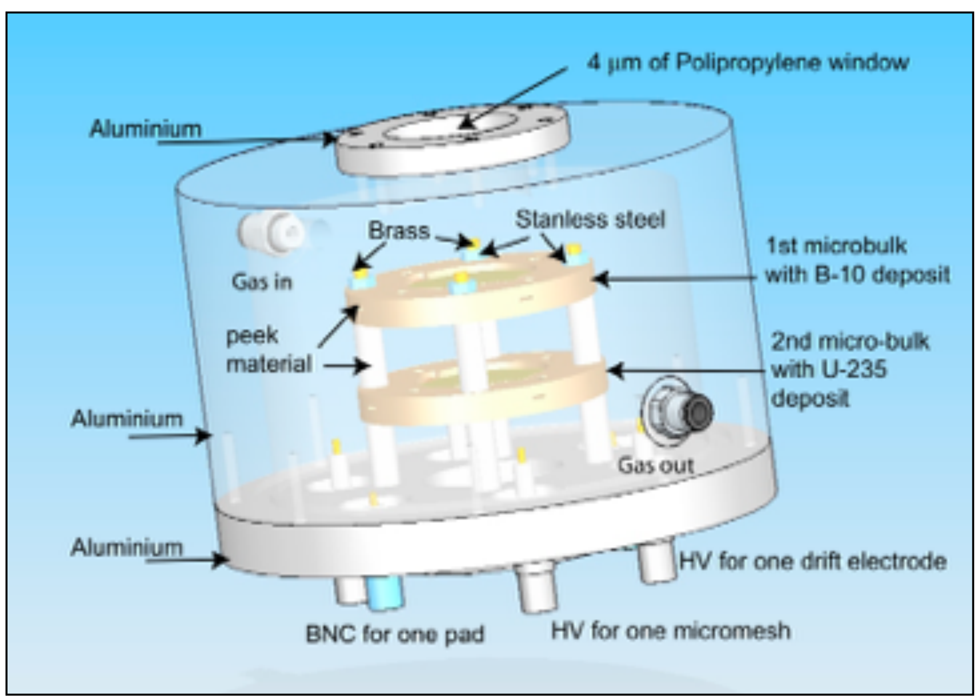

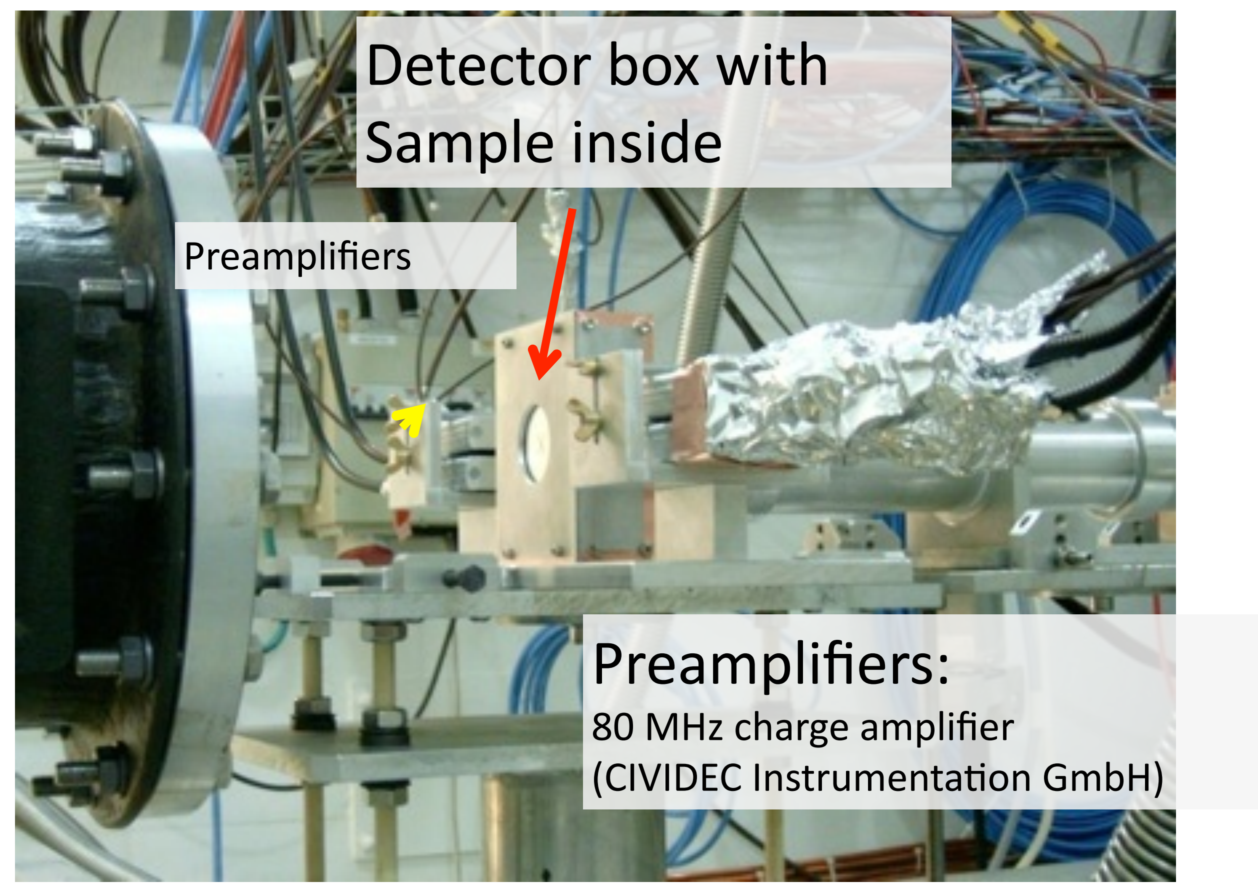

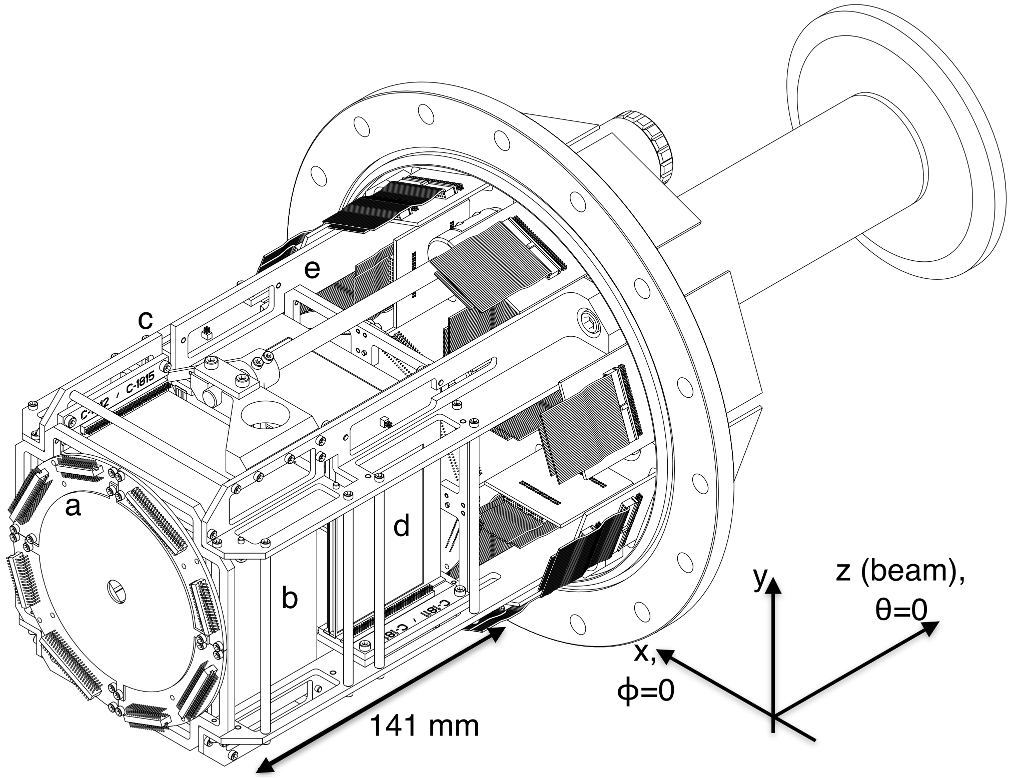

SHARC

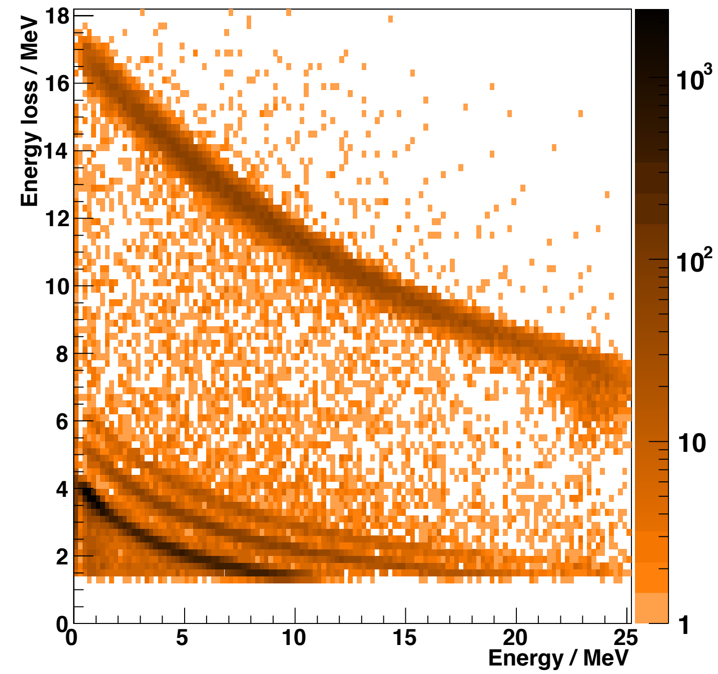

DE-E for 140 um DE detector

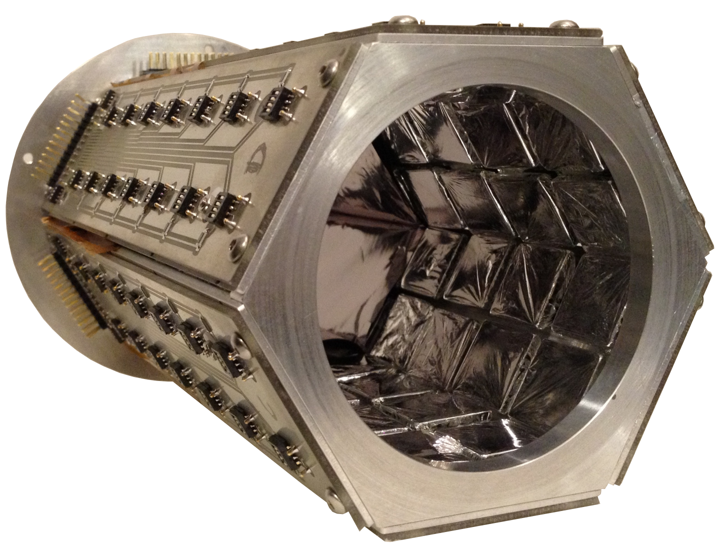

UoYtube - CsI veto tube

Table 2
Model cases used for time dependent calculations.

Case	Outboard blanket module depth	Breeding material	^{6}Li enrichment
1	80 cm	Li_4SiO_4	Natural abundance
2			30%
3			90%
4		Li_2TiO_3	Natural abundance
5			30%
6			90%
7	40 cm	Li_4SiO_4	Natural abundance
8			30%
9			90%
10		Li_2TiO_3	Natural abundance
11			30%
12			90%

Future perspective:
Tritium breeding

- Well constrained for principal production reactions
- How well known are (n,t) reactions on other structural materials?
- Secondary reactions induced by tritons?

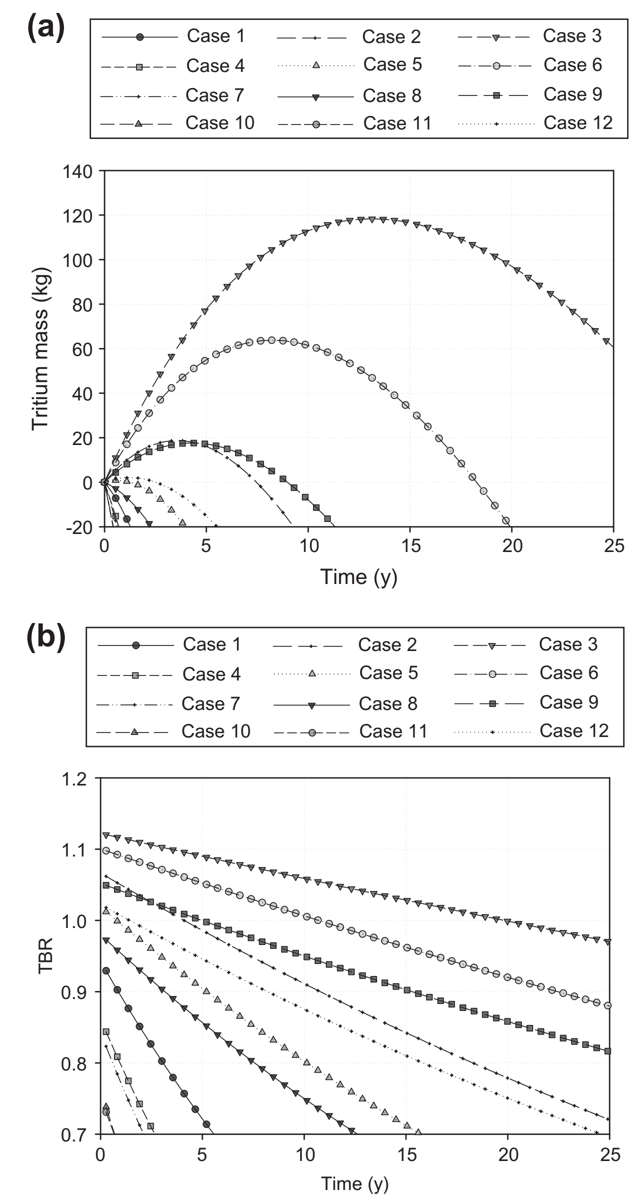

Fig. 3. (a) TBR variation over time and (b) surplus tritium inventory over time for each case. A coverage factor of 0.85 was used.

L.W. Packer et al., J. Nucl. Mat. 417, 718 (2011)

Finis

Main characteristics of the n_TOF neutron beam

- Proton **intensity** *$8x10^{12}$ p/pulse*
- Proton beam **momentum** *20 GeV/c*
- Proton **pulse width** *6 ns (rms)*
- high **instantaneous n flux** *10^5 n/cm^2/pulse*
- wide energy **spectrum** *25 meV$<E_n<$1GeV*
- low **repetition** rate *< 0.25 Hz*
- good energy **resolution** *$\Delta E/E = 10^{-4}$*

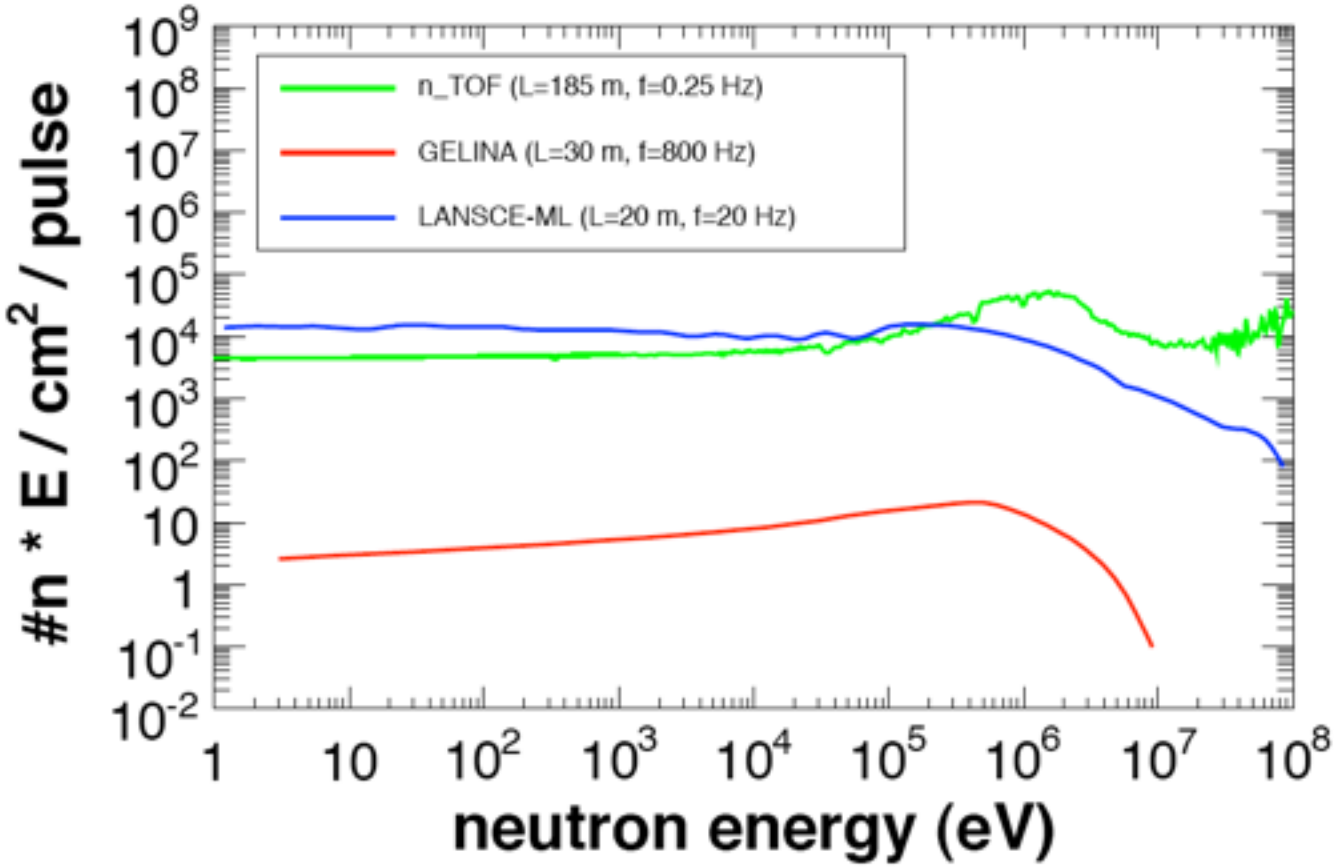

Neutron beam + state-of-the-art detectors and acquisition systems make n_TOF **UNIQUE** for:

- measuring **radioactive isotopes**, in particular **actinides**
- identifying and studying **resonances** (at energies higher than before)
- extending **energy range** for fission (up to 1 GeV !).